UDC 539.21, 53.096

FORMATION OF THE SPECTRAL CONTOUR WIDTH OF NANOPARTICLES PLASMON RESONANCE BY ELECTRON SCATTERING ON PHONONS AND A BOUNDARY SURFACE

Kucherenko M.G., Nalbandyan V.M.

Orenburg State University, Centre of Laser and Information Biophysics, Orenburg, Russia, rphys@mail.osu.ru

The effectiveness of the method of narrowing plasmon resonances of nanoparticles by reducing the temperature was evaluated. It is shown that for particles with a radius of less than 70 nm, it is necessary to take into account the scattering of electrons by the particle surface. This condition significantly limits the possibilities of temperature control of scattering. The data on the transformation of the exciton and plasmon bands of the absorption spectra of spherical layered nanocomposites with the core-shell structure in an external magnetic field are presented. It is shown that the splitting of the plasmon resonance band in a magnetic field can be observed only at electron scattering frequencies below 10^{12} sec^{-1}

Keywords: plasmon resonance, nanoparticle, scattering of electrons, exciton-plasmon interaction

Introduction

As is known, at room temperature the frequency of electron collisions with phonons in different metals and semiconductors takes the values $\sim 10^{13} - 10^{14}\ \text{sec}^{-1}$. However, to observe in the optical frequency range the spectral changes in the polarizabilities of conducting nanoparticles caused by an external magnetic field, it is important that this coefficient does not exceed $10^{11} - 10^{12}\ \text{sec}^{-1}$ [1]. Such a low frequency value γ can be obtained, for example, by lowering the temperature of metals to several tens of kelvins. Only by reducing γ to the required values can one observe the optical manifestations of the influence of an external magnetic field on the physical processes that occur with the participation of metallic nano-objects. These include: absorption and scattering of light, mediated intermolecular nonradiative energy transfer and luminescence near conducting bodies, as well as other similar processes [1].

Quite a large number of works are devoted to the study of electron-phonon collisions in metals and the dependence of various physical phenomena determined by such collisions on temperature. Thus, in [2], the authors investigated individual pure single-crystal silver nanowires (AgNWs) with respect to variations in the characteristics of electrical conductivity, thermal conductivity, and Seebeck coefficient depending on the change in metal temperature from 1.4 K to room temperature. In [3] the electron thermal conductivity of graphene was calculated using various methods by taking into account electron – phonon interactions, including both low-energy, acoustic phonons, and high-energy, optical, and zonal boundary phonons. At low temperatures, the electron thermal conductivity substantially depends on the amount of impurities. However, at room temperature, the impurity effects are small. The authors of [4] studied the contribution of electron-phonon scattering to the electrical conductivity of a quantum cylinder in a longitudinal magnetic field.

1. Experimental installations and measurement techniques

Formulas describing the temperature dependence of the resistance of the nanostructure are obtained in an analytical form, both in the case of the isotropic phonon spectrum and taking into account the effects of the dimensional limitation of phonons. In addition, the authors of this work

investigated the temperature dependence of the conductivity of a quantum cylinder in the case of an isotropic phonon spectrum with a linear dispersion law. It is shown that in the limiting case of relatively low temperatures, the resistance of a quantum cylinder is proportional to the third power of the temperature.

The processes of scattering of conduction electrons are the cause of the electrical resistance of metals. The frequency of electron collisions γ can be determined through the resistivity ρ of the material, using the known formula [5-6]:

$$\gamma = \frac{Ne^2}{m}\rho \ . \tag{1}$$

Here, m and e are the effective mass and electron charge, respectively, N is the effective bulk density of electrons. The resistivity of metals is written as

$$\rho = \frac{m}{Ne^2\tau} = \frac{mv_F}{Ne^2 l}, \tag{2}$$

where v_F is the electron velocity on the Fermi surface, l is the average electron mean free path, and τ is the time between two electron collisions ($\tau = 1/\gamma$).

Two main mechanisms of electron scattering are distinguished:

1) as a result of their collision with local fixed centers – defects, impurities, etc.;

2) as a result of interaction with thermal vibrations of the lattice – phonons.

The effective frequency of collisions consists of two terms – the collision frequencies in the first and second processes, that is, $1/\tau_{eff} = 1/\tau_{prim} + 1/\tau_{phon}$ [5]. This leads to the Mathissen rule.

$$\rho = \rho_{resid} + \rho_{ideal}(T), \tag{3}$$

where ρ_{resid} is the residual resistance, independent of temperature T, associated with the technology of obtaining this metal sample and the quality of its manufacture; $\rho_{ideal}(T)$ is the resistance of the ideal lattice of a given metal due to scattering by phonons with a strong dependence on temperature.

This dependence is described by the Bloch – Gruneisen formula [6]:

$$\rho_{ideal}\left(T/\theta_D\right) = \frac{K_0}{\theta_D}\left(\frac{T}{\theta_D}\right)^5 \int_0^{\theta_D/T} \frac{x^5 dx}{[\exp(x)-1][1-\exp(-x)]} = \frac{K_0}{\theta_D}\left(\frac{T}{\theta_D}\right)^5 J_5\left(\frac{\theta_D}{T}\right), \tag{4}$$

where K_0 is a certain temperature-independent constant characteristic of a given metal, θ_D is the Debye temperature, which determines the maximum oscillation frequency of the grating ($\hbar\omega \cong k_B\theta_D$).

For high temperatures $T/\theta_D \geq 1$, a linear temperature dependence of resistance $\rho_{ideal}(T) \sim T/\theta_D$ (Fig. 1 b) follows from (4), whereas for low temperatures, $T/\theta_D << 1$ a power dependence $\rho_{ideal}(T) \sim (T/\theta_D)^5$ is characteristic (Fig. 1 a).

For metals with a Fermi surface close to spherical, the law $\rho \sim T^5$ has a place already at $T \leq 0.1\theta_D$. For metals with a more complex Fermi surface, this law begins to be satisfied at lower temperatures, when the value of the thermal background pulse becomes smaller than the dimensions of all characteristic Fermi surface features.

Using formula (4) and Table 1, one can obtain the values of the resistivity of the metal and the frequency γ of electron collisions at an arbitrary temperature T. Temperature dependence $\gamma(T)$ can then be represented as

$$\gamma(T)=\gamma(T_0)\left(\frac{T}{T_0}\right)^5\frac{J_5(\theta_D/T)}{J_5(\theta_D/T_0)},\quad J_5(\theta_D/T)=\int_0^{\theta_D/T}\frac{x^5dx}{[\exp(x)-1][1-\exp(-x)]}, \tag{5}$$

where $T_0=293$ K.

As can be seen from the graphs of Fig. 1, the frequency of electron-phonon collisions of different metals takes on the value $\gamma\sim10^{12}$ sec^{-1} at the following temperatures: Au - 30 K, Ag - 40 K, Cu - 54 K, Al - 57 K.

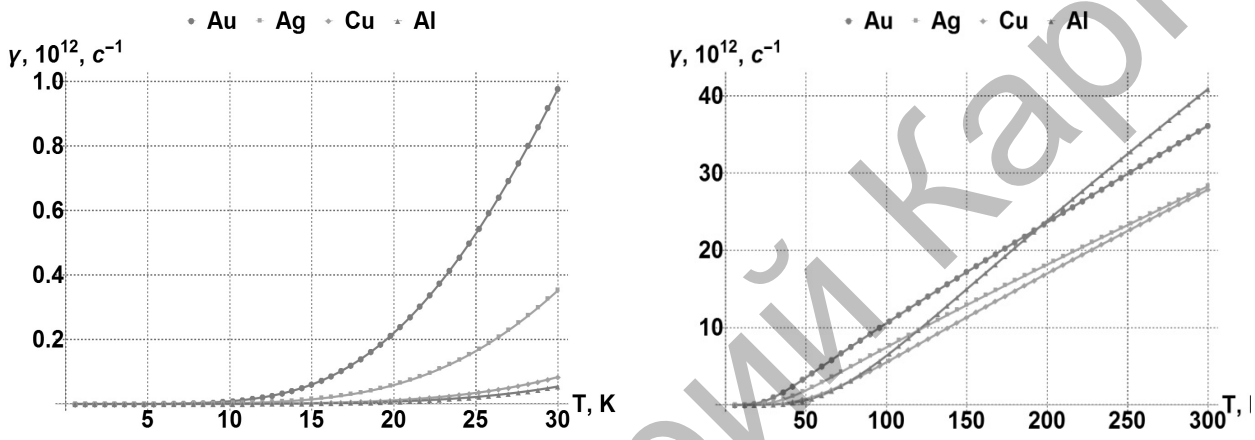

a) temperature range 0-30 K b) temperature range 0-300 K

Fig. 1. The dependence of the frequency γ of electron-phonon collisions for various metals (gold, silver, copper, aluminum) on temperature T.

T a b l e 1. Specific resistances and frequencies γ of pure Cu, Ag, Au and Al at 0° C

Metal	ρ,10^{-6} Ohm· cm	γ,10^{13} sec^{-1}	N_e, 10^{22}, cm^{-3}	m/m_e	θ_D, K
Cu	1.55	2.5	8.5	1.49	344.5
Ag	1.49	2.56	5.86	0.96	225
Au	2.06	3.28	5.6	0.99	165
Al	2.5	3.64	6	1.16	429

In Fig. 2 shows the temperature dependences of the frequency of electron-phonon collisions for various metals in the semi-logarithmic scale in the range of 1–30 K (Fig. 2a) and 1-300 K (Fig. 2b). Already at temperatures above 150 K, the collision frequency γ exceeds the characteristic value $\sim10^{13}$ sec^{-1} for all the metals considered.

In fig. 3a and 3b are shown universal graphs of the temperature dependence of the frequency of electron-phonon collisions, valid for all metals. Relative temperatures T/θ_D are plotted on the horizontal axis, and values for γ are plotted along the vertical axis, without taking into account the characteristic constant related to a particular metal.

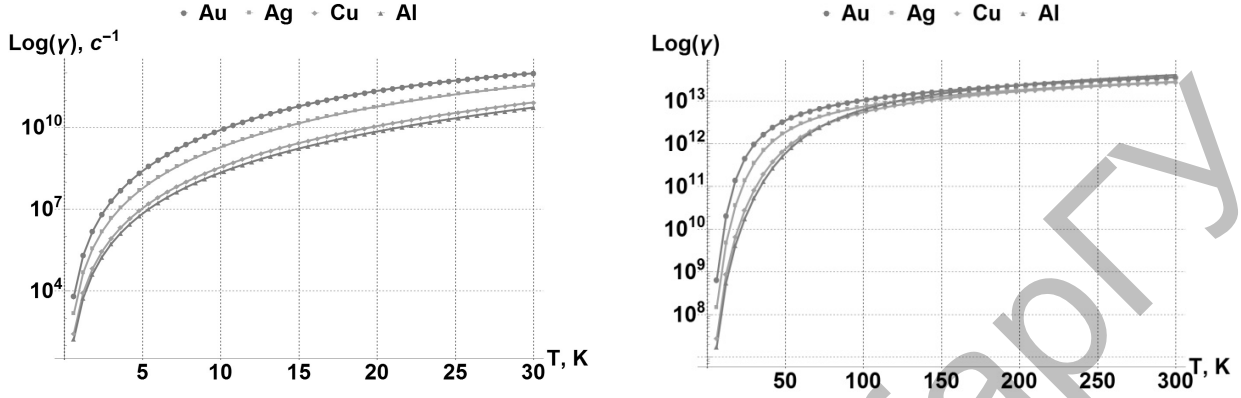

a) temperature range 1-30 K b) temperature range 1-300 K

Fig. 2 The dependence of the collision frequency γ of electrons of different metals (gold, silver, copper, aluminum) on the temperature T on a semi-log scale

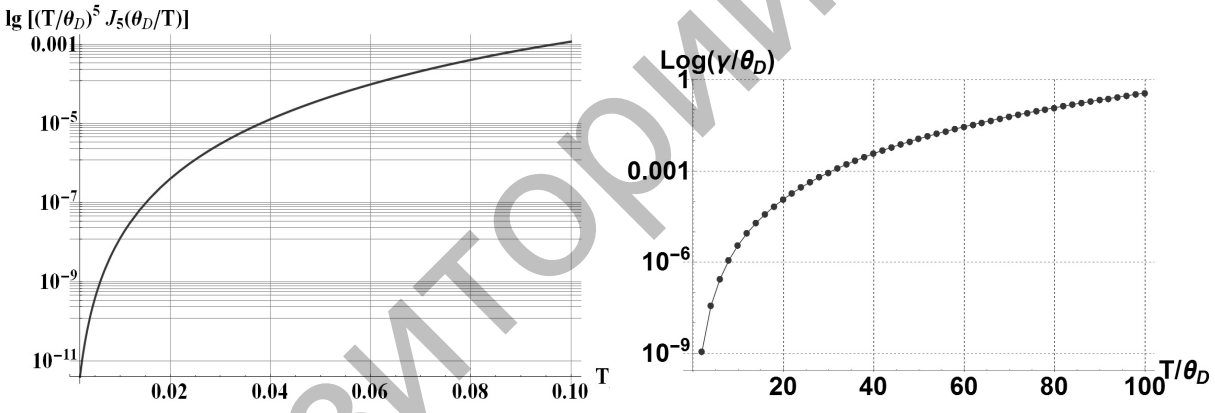

a) b)

Fig. 3. Universal curve of the temperature dependence of the frequency of electron-phonon collisions in the low- (a) and high-temperature (b) intervals

2. Electron collision frequency taking into account scattering by the surface of a nanoparticle. The effect of dimensional dissipation

In the case of conducting nanobodies, apart from the need to take into account the temperature dependence of the frequency of electron-phonon collisions, it is also important to take into account the dependence γ on particle sizes. The expressions considered above for the electron collision frequency were obtained in the framework of the free electron gas relaxation model, which is valid only for macroscopic objects. In the case when the electron mean free path may turn out to be comparable with the size of the particle itself, the scattering of conduction electrons on its surface will lead to a decrease in the relaxation time, i.e. increase in collision frequency. This effect is especially important for nanoparticles, with their high ratio of surface area to volume.

This increase in frequency γ_{sc} caused by the action of the surface is proportional to the Fermi velocity v_F:

$$\gamma_{sc} = Av_F / R,$$

where R is the effective radius of the nanoparticle, A is a parameter describing the degree of loss of coherence when the electron is scattered from the surface.

The frequency γ of total electron scattering in the case of nanoparticles can be represented by an empirical formula [7, 8], in which γ_{bulk} it is defined by formulas (1) and (5):

$$\gamma = \gamma_{bulk} + \gamma_{sc}. \qquad (6)$$

The value of the parameter A for silver and gold lies in the range of $0.1 < A < 0.7$ and $v_F \sim 1{,}4$ nm/fs [9]. In fig. 4 shows the dependence of the electron collision frequency on the radius R (curve 1) and the temperature T (curve 2) of the metal nanoparticle.

Curve (1) fig. 4 corresponds to the frequency of electron scattering by the surface of particles of different radius R, and curve (2) corresponds to the temperature dependence of the frequency of electron-phonon collisions $A = 0.1, v_F = 1.4$ nm / fs. From the analysis of graphs Fig. 4 it can be concluded that it is impossible to reduce the frequency γ of electron collisions to arbitrary values by lowering the temperature of the metal. When a certain value is reached, the first component in (6) becomes smaller than the second ($\gamma_{bulk} < \gamma_{sc}$), which is responsible for the scattering of electrons on the surface of a particle. Then the main contribution to the scattering will make γ_{sc}. Therefore, a further decrease γ_{bulk} caused by the cooling of the metal no longer contributes to a decrease in the overall frequency γ.

For example, for a gold nanoparticle with a radius of 70 nm (Fig. 4), the collision frequency at which the scattering on the surface becomes more significant than the electron-phonon scattering at a temperature $T = 35$ K is $\gamma \sim 2 \cdot 10^{12}$ sec^{-1}. A decrease in the frequency γ leads to an increase in the resolution of the lines of the optical absorption spectrum by nanoparticles (Fig. 5).

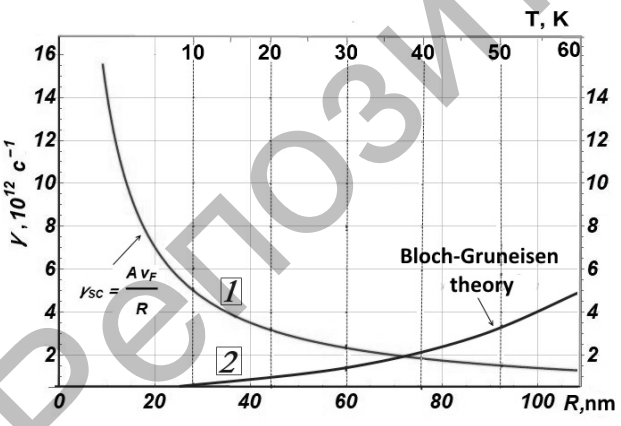

Fig. 4 Dependence of the frequency of electron collisions on the temperature and radius of metal nanoparticles: 1 - dependence of the electron scattering frequency by the particle surface on its radius R; 2 - temperature dependence of the frequency of electron-phonon collisions in a pure metal.

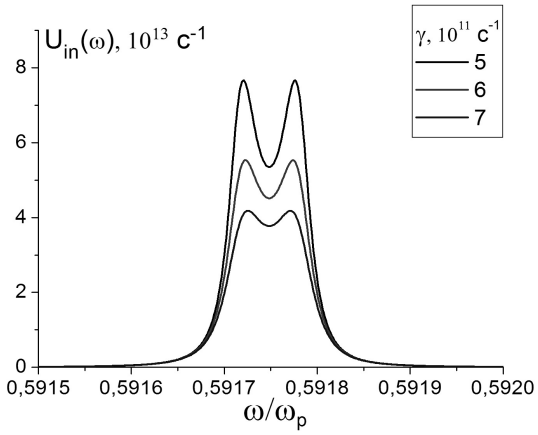

Fig. 5 Splitting of the spectrum of the absorption rate $U_{in}(\omega)$ of the energy of the electromagnetic field in a spherical layered nanocomposite with a magnetized conducting core and excitonogenic shell depending on the magnitude of the plasmon damping coefficient γ.

3. Spectra of nanocomposites with exciton-plasmon interaction

The effect of metallic nanoparticles on various processes sensitive to plasmon resonance has been studied in sufficient detail. In recent years, much attention has been given to the participation of molecular excitons in processes that are developed in metal composite complexes [11–13]. At the next stage of nanotechnology development, it is of interest to study the phenomena that can be caused by the exciton-plasmon interaction. In [14] the effects of plasmon-exciton interaction in the absorption and scattering of light by hybrid nanoparticles consisting of a metal core and a J-aggregate shell of an organic dye were studied. The spectral characteristics of the particles were calculated for two concentric spheres within the framework of the generalized Mie theory in a wide range of wavelengths and geometric parameters of the system for various core materials (Ag, Au, Cu, Al) and the cyanine dye shell (TC, OC and PIC). The eigen frequencies of the hybrid modes of the system and the intensities of the photo absorption peaks are determined. Their dependences on the oscillator strength of the transition in the J-band of the dye, the core radius and the shell thickness are examined. A qualitatively different character of the effect of the interaction of the Frenkel exciton with dipole and multipole plasmons on the optical properties of the composite nanoparticles under study is demonstrated. It is shown that by varying the sizes and optical constants of the materials of the particle, the total number of spectral peaks changes and a significant redistribution of their intensities occur at the maxima. The dominant regions of the processes of absorption and scattering of light in the extinction spectra are found.

The interaction of molecular excitons in organic films with a metal substrate was investigated in [15]. In another paper [16], the authors considered an exciton-plasmon interaction in a three-layer spherical nanocomposite consisting of a metal core (Au) covered by two layers of an organic dye. The first layer of the dye is needed to maintain the connection of plasmons with excitons. The photoluminescence spectrum of the composite obtained in this work contained the narrow-band peak of the J-aggregates, which was amplified locally by plasmons.

In paper [17] dipole polarizabilities and absorption cross sections of two-particle nanoclusters of conductive homogeneous and layered particles with the degenerate electron gas was considered. Frequency dependences of the dipole polarizabilities of clusters consisting of two solid conducting spherical nanoparticles and double-layer metal nanoparticles are investigated versus the geometrical parameters of the system with taking into account the degeneracy of electron gas of its metallic components. It is established that the spectra of the dynamic polarizabilities and absorption cross-sections of clusters have a complex multi resonant structure and strong dependence on the configuration parameters of the cluster, the degree of degeneracy of the metal, and kinetic characteristics of its electron gas. Spectral transformations of the absorption cross-sections of nanoclusters are illustrated under variation of the radii of particles or theirs nuclei, characteristic lengths of the Thomas-Fermi screening, and frequency of electron collisions. The anisotropic nature of absorption of electromagnetic field energy by a cluster is established: it is shown that the value of the absorption cross section depends on the direction of the electric field strength vector relative to the axis of the cluster.

We investigated the exhibition of the exciton-plasmon interaction in spherical layered nanocomposites with the metal core – crystal-like molecular shell structure. Figure 6 shows the spectra of the absorption rate of the field energy in the exciton-envelope depending on the magnitude of the induction of the external magnetic field at a zero plasmon attenuation coefficient $\gamma = 0$ (Fig. 6a), i.e. without taking into account the energy absorption by the metal core, and the attenuation coefficient of the plasmons $\gamma = 6 \cdot 10^{11} \sec^{-1}$ (Fig. 6b).

The graphs show that the plasmon resonance in a magnetic field increases in amplitude and splits into two spectral lines, scattering in the region of high and low frequencies with increasing magnetic induction *B*. At the same time, the effect of the magnetic field on the exciton resonances is small (exciton bands not shown in the figure). When taking into account the field energy absorption

by the metal core of a layered nanocomposite, i.e. when, plasmon resonances broaden and their amplitude decreases by two orders of magnitude. The resonance splitting is observed at the magnetic induction value B = 10 T, and an increase in the magnetic induction affects the amplitude of the plasmon resonance, just as with a zero plasmon damping coefficient, i.e. the speed of light absorption in a magnetic field increases, which is reflected in the graphs shown in Figure 6b.

The absorption speed in the volume dV of the excitonogenic layer with coordinates r,θ is determined by the square of the modulus of the local field strength vector $\left|\mathbf{E_2}(\omega,r,\theta)\right|^2$ inside the layer and will have the following form [10]

$$dU_{in}(\omega,r,\theta)=\frac{1}{2\pi\hbar}\operatorname{Im}\varepsilon_2(\omega)\left|\mathbf{E_2}(\omega,r,\theta)\right|^2 dV\,, \tag{7}$$

where $\varepsilon_2(\omega)$ is the dielectric constant of the crystal-like excitonogenic layer is determined by the expression [18]

$$\varepsilon(\mathbf{k},\omega)=\varepsilon_0-\frac{f^2}{[\omega+i\Gamma(\omega,\mathbf{k})]^2-\omega_{res}^2(\mathbf{k})}\,, \tag{8}$$

and ε_0 is the dielectric constant due to all other states of electrons, except for the exciton states; $\Gamma(\omega,\mathbf{k})\equiv\gamma(\mathbf{k},\omega)+\eta$ is the relaxation rate due to the interaction of excitons with phonons; factor $f^2\equiv\Omega_p^2F$ characterizes the connection of photons with excitons; $\Omega_p^2\equiv 4\pi e^2/mv$ is the square of the "plasma frequency"; $F\equiv 2\omega_f md^2/\hbar e^2$ is the oscillator strength of a transition; $\omega_{res}(\mathbf{k})=\omega(\mathbf{k})+\Delta(\mathbf{k},\omega)$ is the frequency of excitons renormalized due to interaction with phonons.

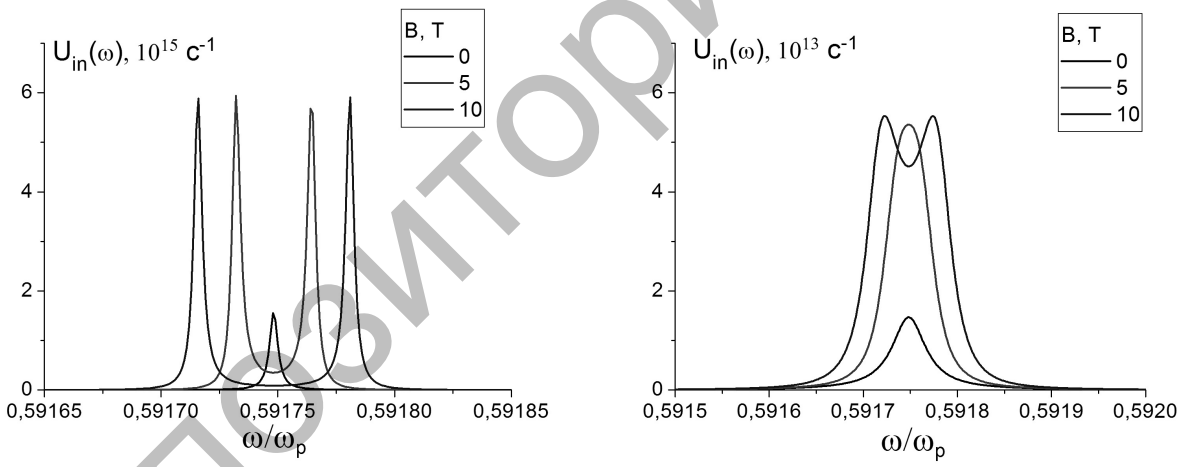

a) $\gamma=0$ b) $\gamma=6\cdot10^{11}\,\mathrm{sec}^{-1}$

Fig.6. Spectra of the rate of field energy absorption in the excitonogenic shell of a layered on-nanocomposite with a magnetized core, depending on the magnitude of the magnetic induction with a zero-left plasmon attenuation coefficient $\gamma=0$ (a) and (b) plasmon attenuation coefficient $\gamma=6\cdot10^{11}\,\mathrm{sec}^{-1}$.

Thus, the dielectric constant of molecular J-aggregates is a complex function with spatial and frequency dispersion. In this work, only the frequency dispersion for the zero exciton wave vector **k** = 0 was taken into account. The vector of the electric field strength inside the excitonogenic layer of the shell was represented as

$$\mathbf{E_2}(r,\theta\,|\,\omega)=-\vec{\nabla}\left[-\vec{\vec{\mathbf{C}}}(\vec{\varepsilon}_1,\varepsilon_2,\varepsilon_3)\mathbf{E_0}\mathbf{r}+\vec{\vec{\mathbf{D}}}(\vec{\varepsilon}_1,\varepsilon_2,\varepsilon_3)\mathbf{E}_0\frac{\mathbf{r}}{r^3}\right], \tag{9}$$

where $\vec{\vec{C}}, \vec{\vec{D}}$ are transformational tensors, expressions for which are given in [10].

Two or three exciton resonances should appear in the spectra, two of which are due to the square of the magnitude vector of the intensity $|\mathbf{E_2}(\omega, r, \theta)|^2$, and the third to the multiplier $\mathrm{Im}\,\varepsilon_2(\omega)$. However, this resonance did not manifest itself in the calculated spectra, since it merged with one of the two other exciton resonances. In addition, there is a plasmon resonance in the spectrum, even with a zero plasmon damping coefficient $\gamma = 0$, i.e. when the absorption of the field energy by the metal core does not take place. Expression for the rate of field energy absorption by the entire layered spherical nanocomposite

$$U(\omega | B) = \frac{1}{2\hbar} \mathrm{Im}[\mathbf{E}_0^* \vec{\vec{\mathbf{A}}}(\omega | B)\mathbf{E}_0], \tag{10}$$

where the dipole polarizability tensor of a layered spherical composite with a magnetized core is determined by the expression [10]

$$\begin{aligned} &\vec{\vec{\mathbf{A}}}(\vec{\vec{\varepsilon}}_1(\omega | \mathbf{B}), \varepsilon_2(\omega), \varepsilon_3) = \\ &= [(\vec{\vec{\varepsilon}}_1(\omega | \mathbf{B}) + 2\varepsilon_2(\omega))(\varepsilon_2(\omega) - \varepsilon_3) + (\vec{\vec{\varepsilon}}_1(\omega | \mathbf{B}) - \varepsilon_2(\omega))(2\varepsilon_2(\omega) + \varepsilon_3)\xi^3] \times \\ &\times [(\vec{\vec{\varepsilon}}_1(\omega | \mathbf{B}) + 2\varepsilon_2(\omega))(\varepsilon_2(\omega) + 2\varepsilon_3) + 2(\vec{\vec{\varepsilon}}_1(\omega | \mathbf{B}) - \varepsilon_2(\omega))(\varepsilon_2(\omega) - \varepsilon_3)\xi^3]^{-1} R_2^3. \end{aligned} \tag{11}$$

An alternative model for the formation of the field energy absorption spectra of the entire layered nanocomposite is based on expression (10). In the spectra calculated on the basis of (10), as before, three resonances manifest themselves - two exciton in the low-frequency region of the spectrum and one plasmon in the high-frequency region.

Conclusion

Thus, the limiting factor for the temperature decrease in the frequency of electron collisions in a metal is the effect of electron scattering by the nanoparticle surface. Thus, a decrease in the nanoparticle radius to $R < 10 \div 15$ nm values leads to a sharp increase in the frequency γ_{sc} by an order of magnitude ($\gamma \sim 10^{13}\,\mathrm{sec}^{-1}$), which makes the temperature method of increasing the relaxation time of electrons in small metal bodies of small size ineffective. To perform high-resolution spectral optical measurements for systems containing conducting nanoparticles, joint optimization of geometric and thermodynamic parameters is necessary (Fig. 4). In fact, the critical value of the nanoparticle radius at which electron scattering by the surface makes a contribution comparable to electron to phonon scattering at a temperature T = 35 K is a radius of about 70 nm. Although the problem of enhanced resolution of the optical spectra of plasmon nanoparticles was associated with the detection of magnetic effects, in this work we did not consider the possible influence of a magnetic field on the frequency of collisions of electrons with the surface of the nanoparticle. It is expected that in strong fields the frequency of such collisions will decrease due to the curvature of the ballistic electron trajectory. Then, spectral measurements with plasmon nanostructures in a magnetic field can have an improved resolution as the temperature decreases to the subcritical region due to the magnetic suppression of surface scattering. This can contribute to the achievement of the optimal value of the frequency γ of collisions of electrons with phonons of the order $10^{11}\,\mathrm{sec}^{-1}$.

Acknowledgements

The work was done by funding the Ministry of Education and Science of the Russian Federation (Minobrnauka) (3.7758.2017/BCh).

REFERENCES

1 Kucherenko M.G., Nalbandyan V.M. Absorption and spontaneous emission of light by molecules near metal nanoparticles in external magnetic field. *Physics Procedia*, 2015, Vol. 73, pp. 136 – 142.

2 Kojda D. et al. Temperature-dependent thermoelectric properties of individual silver nanowires. Temperature-dependent thermoelectric properties of individual silver nanowires. *Physical Review B*. 2015. Vol. 91, pp. 024302.

3 Kim T.Y., Cheol-Hwan Park, Marzar N. The electronic thermal conductivity of grapheme. *Nano. Lett*. 2016, pp. 1 – 15.

4 Eminov P.A., Ul'din A A, Sezonov Yu.I. Electron-phonon scattering and conductivity of a quantum cylinder in a magnetic field. *Physics of the Solid State*, 2011, Vol. 53, No. 8, pp. 1707–1713.

5 Babichev A.P., Babushkina N.A., Bratkovskii A.M., et al. *Physical values*. Handbook Energoatomizdat. Moskow, Russian, 1991, 1232 p. [in Russian]

6 Ziman J.M. *Electrons and Phonons. Theory of Transport Phenomena in Solids*. Oxford: Clarendonpress, 1960, 554 p.

7 Genzel L. Dielectric function and infrared absorption of small metal particles. *Zeitschriftfür Physik B Cond. Matter*. 1980, Vol. 37, pp. 93 – 101.

8 Kawabata A., Kubo R. Electronic properties of fine metallic particles. II. Plasma resonance absorption. *Jour. Phys. Soc. Japan*. 1966, Vol. 21, pp. 1765 – 1722.

9 Persson B.N.J. Polarizability of small spherical metal particles: influence of the matrix environment. *Surface Science*. 1993, Vol. 281, pp. 153 – 162.

10 Kucherenko M.G., Nalbandyan V.M. Polarizability spectra of magnetized layered nanocomposites with an anisotropic core or cladding and localized surface plasmons. *Journal of Optical Technology*. 2018, Vol. 85, Issue 9, pp. 524 – 530.

11 Saikin S.K., Eisfeld A., Valleau S., Aspuru-Guzik A. Photonics meets excitonics: natural and artificial molecular aggregates. *Nanophotonic*s, 2013, Vol. 2, No. 1, pp. 21 – 38.

12 Sun Y., GiebinkN.C., Kanno H., Ma B., Thompson M.E., Forrest R. Management of singlet and triplet excitons for efficient white organic light-emitting devices. *Nature*. 2006, Vol. 440, No. 7086, pp. 908 – 912.

13 Vielma J., Leung P.T. Nonlocal optical effects on the fluorescence and decay rates for admolecules at a metallic nanoparticle. *The Journal of chemical physics*. 2007, Vol. 126, No. 19, pp. 194704.

14 Lebedev V.S., Medvedev A.S. Plasmon-exciton coupling effects in light absorption and scattering by metal/J-aggregate bilayer nanoparticles. *Quantum electron*. 2012, No. 42(8), pp. 701 – 713.

15 Azarova N., Ferguson A., Jao van de Lagemaat, Rengnath E., Park W., Johnson J.C. Coupling between a Molecular-Transfer Exciton and Surface Plasmons in a Nanostructured Metal Grating. *Journal of Physical Chemistry Lett*ers. 2013, Vol. 4, No. 16, pp. 2658 – 2663.

16 Vasil'ev D.N., Koltsova E.S., Chubin D.A. Effect of the plasmon-exciton interaction on optical properties of core-shell nanoparticle. *Bulletin of the Lebedev Physics Institute*. 2010, Vol. 37, No. 3, pp. 87 – 88.

17 Kucherenko M.G., Nalbandyan V.M. Dipole Polarizabilities and Absorption Cross Sections of Two-Particle Nanoclusters of Conductive Homogeneous and Layered Particles with the Degenerate Electron Gas. *Russian Physics Journal*. 2017, Vol. 59, Issie 9, pp. 1425 – 1432.

18 Davydov A.S., Mjasnikov E.N. Absortion and dispertion of light by molecular excitons. *Phys. stat. sol*., 1967, Vol. 20, pp. 153.

Article accepted for publication 05.11.2018